SRG operator evolution

A. J. Tropiano[1], S. K. Bogner[2], R. J. Furnstahl[1]

[1]*Department of Physics, The Ohio State University, Columbus, OH 43210, USA*

[2]*National Superconducting Cyclotron Laboratory and Department of Physics and Astronomy, Michigan State University, East Lansing, MI 48824, USA*

(Dated: May 31, 2019)

Abstract

Brief description of project.

CONTENTS

I. INTRODUCTION

Results on SRG-evolved operators from several NN potentials:
– How operators evolve from band- and block-diagonal SRG transformations.
– Operator evolution for different potentials (regulators, chiral order, etc.)

II. MATHEMATICAL/COMPUTATIONAL DETAILS

A. Building SRG unitary transformations

Brief description of how to make $U(s)$.

Diagonalize initial and evolved Hamiltonians which we will call $H(0)$ and $H(s)$, respectively. This gives $\psi_\alpha(0)$ and $\psi_\alpha(s)$ for each eigenvalue indexed by α. Then the SRG unitary transformation can be computed by taking a sum over outer products of the evolved and initial wave functions:

$$U(s) = \sum_{\alpha=1}^{N} |\psi_\alpha(s)\rangle \langle\psi_\alpha(0)| \,, \tag{1}$$

where N is the dimension of the Hamiltonian matrix. Here the weights are factored into the wave functions, thus $U(s)$ is unitless.

To evolve operators, we simply apply $U(s)$:

$$O(s) = U(s)O(0)U^\dagger(s), \tag{2}$$

where $O(0)$ is the bare operator.

B. Momentum projection operator: $a_q^\dagger a_q$

C. Momentum distribution function: ϕ^2

III. RESULTS

Organize this according to the figures: what story do the figures tell? Format should be description of the calculation, followed by the figure, followed by takeaways.

A. Entem-Machleidt N^{3}LO non-local potential

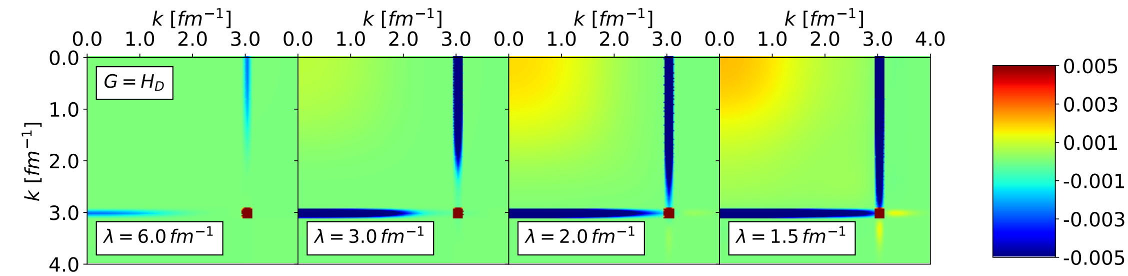

(a)

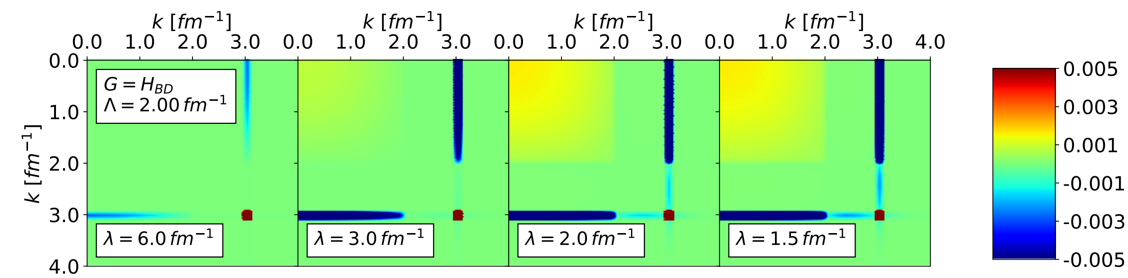

(b)

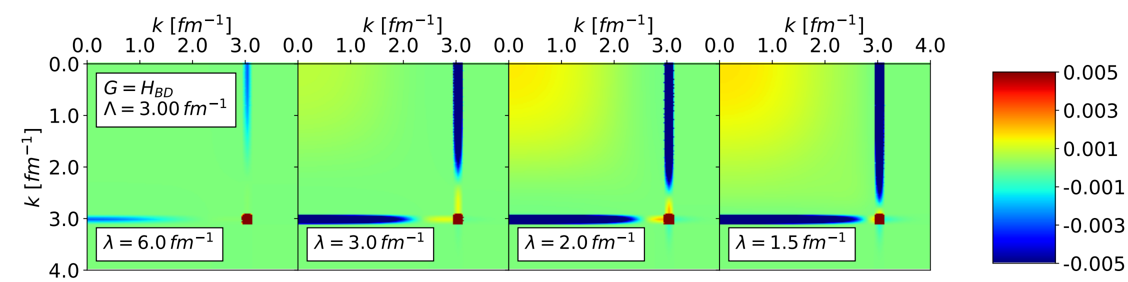

(c)

FIG. 1: Matrix elements of $\langle k|a_q^\dagger a_q|k'\rangle$ SRG-evolving in λ right to left under transformations from the Entem-Machleidt N^{3}LO non-local potential with the Wegner generator (a) and block-diagonal generators decoupling at $\Lambda = 2$ and 3 fm^{-1} (b and c). Here $q = 3$ fm^{-1}.

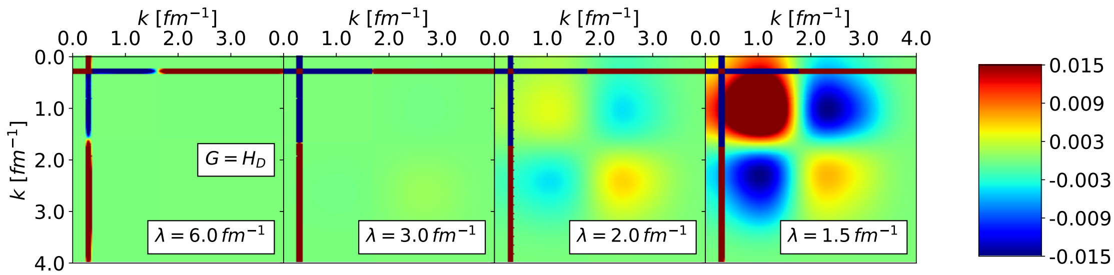

FIG. 2: Matrix elements of $\langle k|a_q^\dagger a_q|k'\rangle$ SRG-evolving in λ right to left under transformations from the Entem-Machleidt N^{3}LO non-local potential with the Wegner generator. Here $q = 0.3$ fm^{-1}.

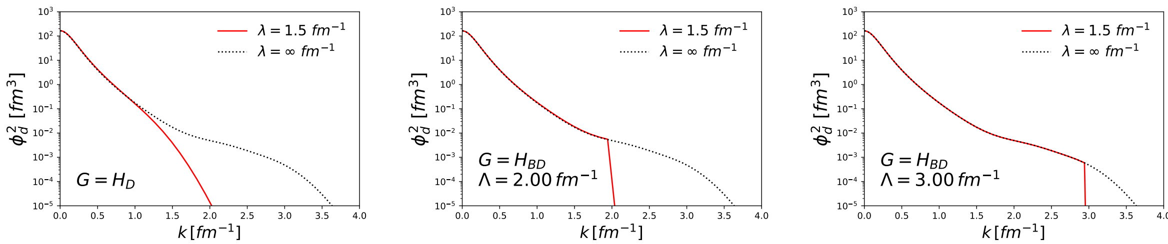

(a) (b) (c)

FIG. 3: Momentum probability densities of the deuteron SRG-evolving the wave function to $\lambda = 1.5$ fm^{-1} from the Entem-Machleidt N^{3}LO non-local potential with the Wegner generator (a) and block-diagonal generators decoupling at $\Lambda = 2$ and 3 fm^{-1} (b and c). The black dotted line corresponds to the momentum probability density of the initial deuteron wave function.

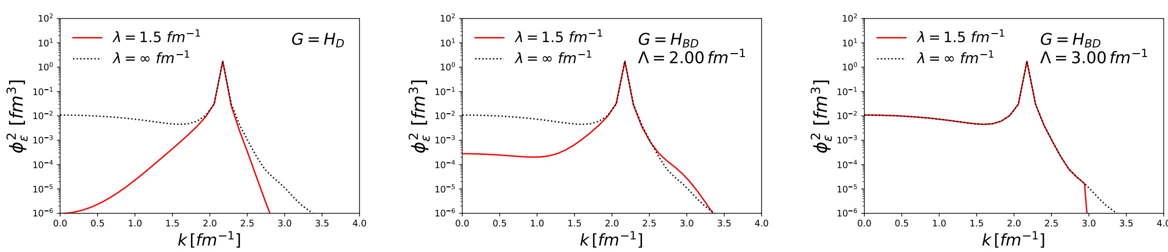

(a) (b) (c)

FIG. 4: Momentum probability densities of the continuum state at $\epsilon \approx 200$ MeV SRG-evolving the wave function to $\lambda = 1.5$ fm^{-1} from the Entem-Machleidt N^{3}LO non-local potential with the Wegner generator (a) and block-diagonal generators decoupling at $\Lambda = 2$ and 3 fm^{-1} (b and c). The black dotted line corresponds to the initial momentum probability density.

B. RKE N^{3}LO and N^{4}LO semi-local potentials

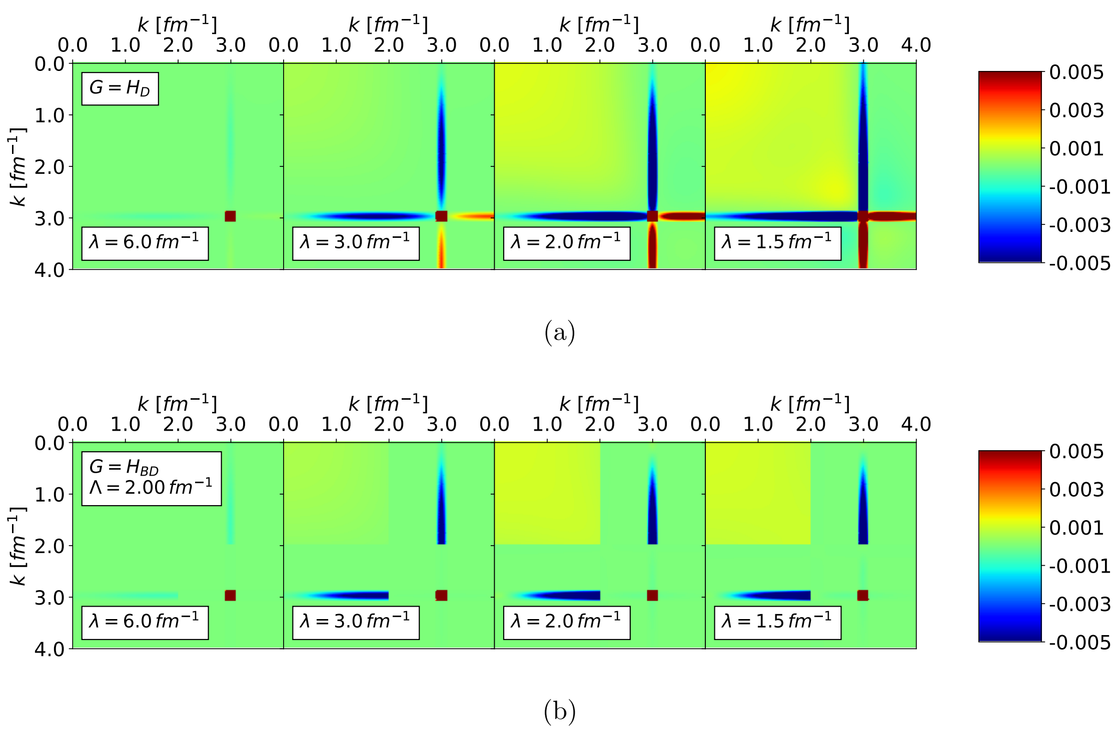

FIG. 5: Matrix elements of $\langle k|a_q^\dagger a_q|k'\rangle$ SRG-evolving in λ right to left under transformations from the RKE N^{3}LO semi-local potential with the Wegner generator (a) and block-diagonal generator decoupling at $\Lambda = 2$ fm^{-1} (b). Here $q = 3$ fm^{-1} and the EFT cutoff is 450 MeV.

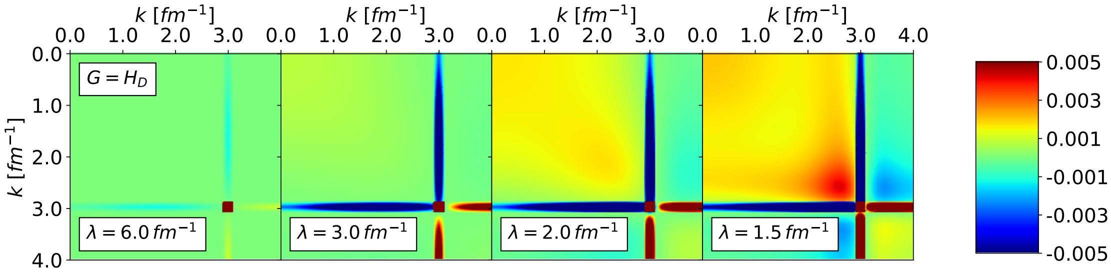

(a)

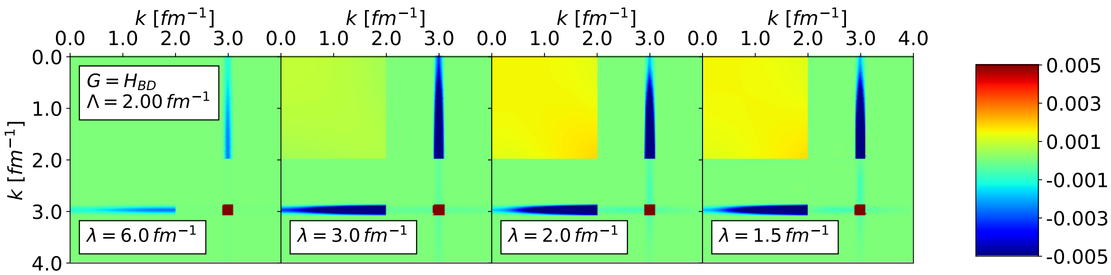

(b)

FIG. 6: Matrix elements of $\langle k|a_q^\dagger a_q|k'\rangle$ SRG-evolving in λ right to left under transformations from the RKE N^{3}LO semi-local potential with the Wegner generator (a) and block-diagonal generator decoupling at $\Lambda = 2$ fm^{-1} (b). Here $q = 3$ fm^{-1} and the EFT cutoff is 500 MeV.

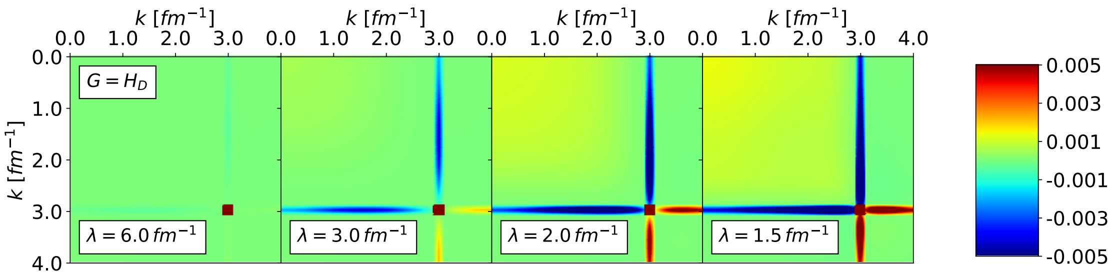

(a)

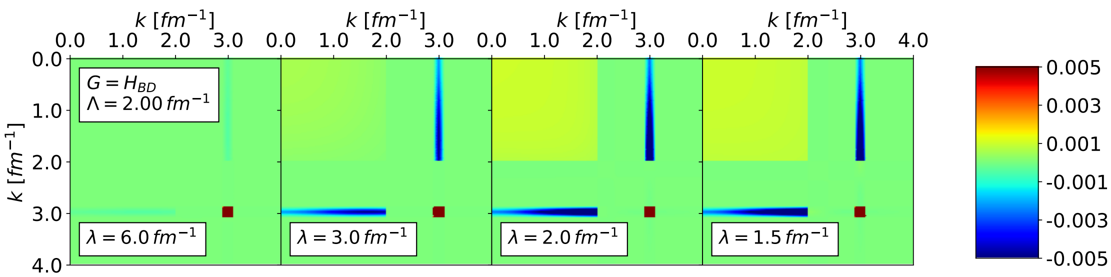

(b)

FIG. 7: Matrix elements of $\langle k|a_q^\dagger a_q|k'\rangle$ SRG-evolving in λ right to left under transformations from the RKE N^{4}LO semi-local potential with the Wegner generator (a) and block-diagonal generator decoupling at $\Lambda = 2$ fm^{-1} (b). Here $q = 3$ fm^{-1} and the EFT cutoff is 450 MeV.

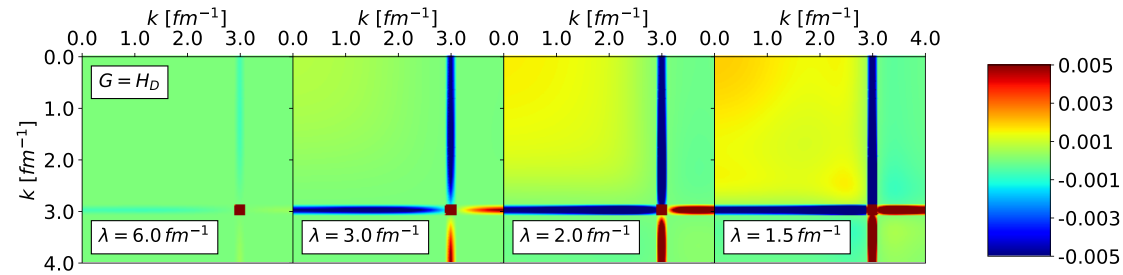

(a)

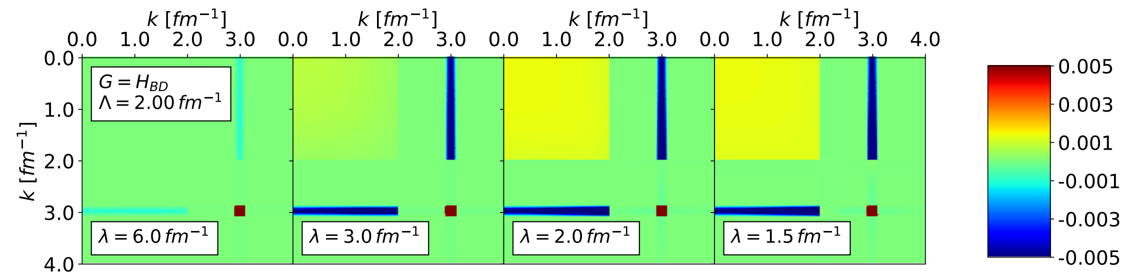

(b)

FIG. 8: Matrix elements of $\langle k|a_q^\dagger a_q|k'\rangle$ SRG-evolving in λ right to left under transformations from the RKE N^{4}LO semi-local potential with the Wegner generator (a) and block-diagonal generator decoupling at $\Lambda = 2$ fm^{-1} (b). Here $q = 3$ fm^{-1} and the EFT cutoff is 500 MeV.

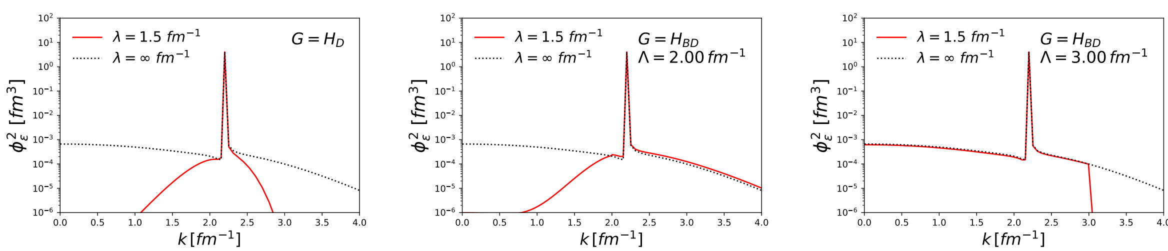

(a) (b) (c)

FIG. 9: Momentum probability densities of the continuum state at $\epsilon \approx 200$ MeV SRG-evolving the wave function to $\lambda = 1.5$ fm^{-1} from the RKE N^{4}LO semi-local potential with the Wegner generator (a) and block-diagonal generators decoupling at $\Lambda = 2$ and 3 fm^{-1} (b and c). The black dotted line corresponds to the initial momentum probability density. Here the EFT cutoff is 450 MeV.

C. Gezerlis N^{2}LO local potentials

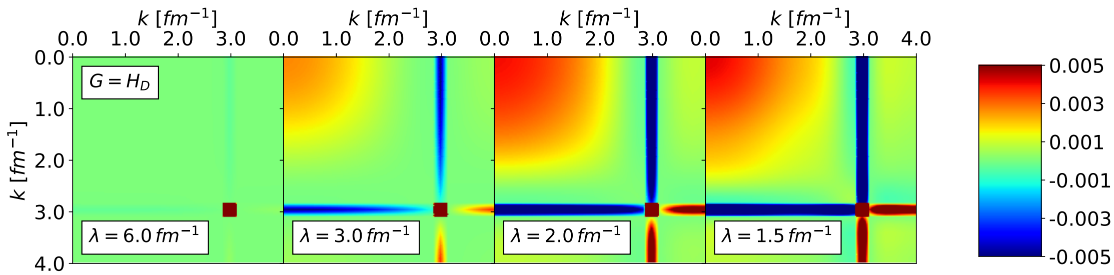

(a)

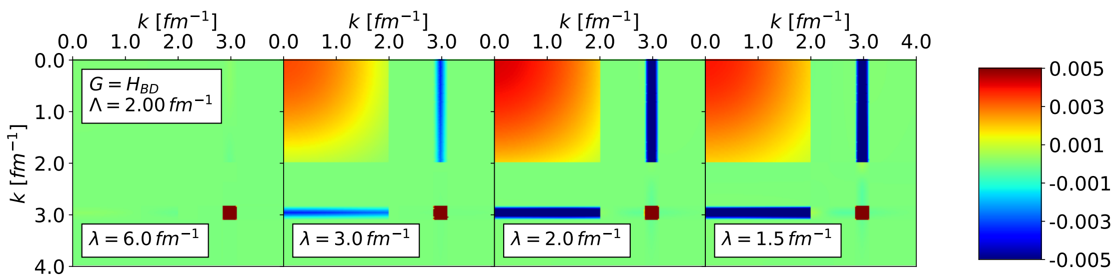

(b)

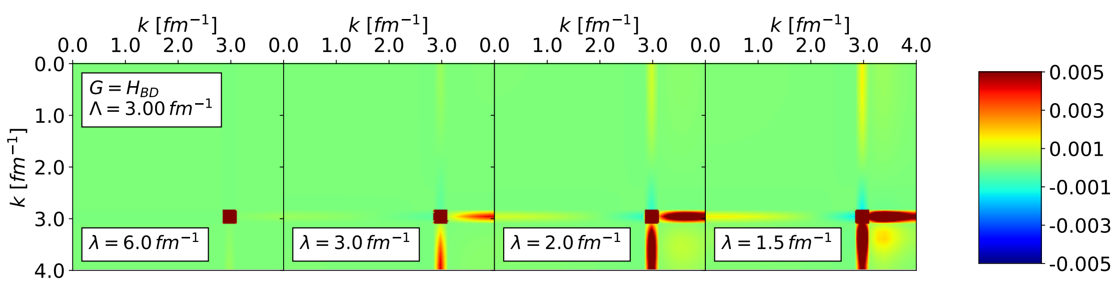

(c)

FIG. 10: Matrix elements of $\langle k|a_q^\dagger a_q|k'\rangle$ SRG-evolving in λ right to left under transformations from the Gezerlis et al. N^{2}LO local potential with the Wegner generator (a) and block-diagonal generators decoupling at $\Lambda = 2$ and 3 fm^{-1} (b and c). Here $q = 3$ fm^{-1} and the EFT cutoff is 1 fm.

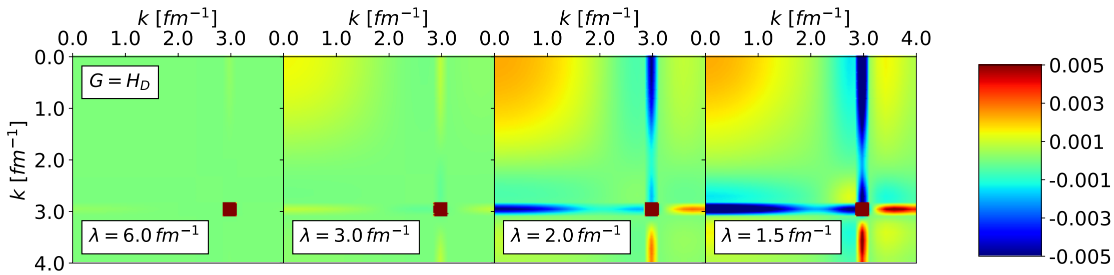

(a)

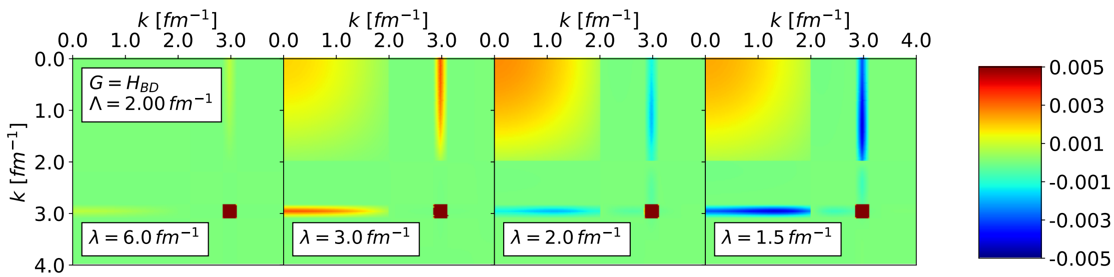

(b)

FIG. 11: Matrix elements of $\langle k|a_q^\dagger a_q|k'\rangle$ SRG-evolving in λ right to left under transformations from the Gezerlis et al. N^{2}LO local potential with the Wegner generator (a) and block-diagonal generator decoupling at $\Lambda = 2$ fm^{-1} (b). Here $q = 3$ fm^{-1} and the EFT cutoff is 1.2 fm.

[1] D. R. Entem and R. Machleidt, Phys. Rev. C **68**, 041001 (2003), arXiv:nucl-th/0304018 [nucl-th].

[2] P. Reinert, H. Krebs, and E. Epelbaum, Eur. Phys. J. A **54**, 86 (2018), arXiv:1711.08821 [nucl-th].

[3] A. Gezerlis, I. Tews, E. Epelbaum, M. Freunek, S. Gandolfi, K. Hebeler, A. Nogga, and A. Schwenk, Phys. Rev. C **90**, 054323 (2014), arXiv:1406.0454 [nucl-th].